Int. J. Electrochem. Sci., 13 **(2018)** 3613 – 3624, doi: 10.20964/2018.04.51

International Journal of
ELECTROCHEMICAL
SCIENCE
www.electrochemsci.org

Electrochemical and Corrosion Behavior of 316L Stainless Steel in a CO_2-SO_2-H_2O Mixture

Yong Xiang[1,2,*], *Chen Li*[1,2], *Zhengwei Long*[1,2], *Canwen Zhang*[1], *Zhongli Ji*[1,2]

[1] College of Mechanical and Transportation Engineering, China University of Petroleum, Beijing 102249, China
[2] Beijing Key Laboratory of Process Fluid Filtration and Separation, China University of Petroleum, Beijing 102249, China
[*]E-mail: xiangy@cup.edu.cn

Received: 15 December 2017 / *Accepted:* 10 February 2018 / *Published:* 6 March 2018

Although steel corrosion in a SO_2-containing atmospheric environment has been extensively investigated, its electrochemical behavior still needs to be addressed, especially when it coexists with CO_2 in a carbon capture, utilization and storage system. In this work, electrochemical experiments with 316L stainless steel corrosion in a CO_2-saturated solution were conducted by adding different amounts of SO_2 to a solution at 25 °C under different pH conditions. The effect of SO_2 on the cathodic reactions of 316L stainless steel corrosion in a CO_2-saturated solution was investigated by electrochemical methods, including potentiodynamic sweep, linear polarization resistance and electrochemical impedance spectroscopy. The results showed that the presence of SO_2 increased the cathodic limiting current and corrosion rates of 316L stainless steel at the same pH. There was a "second-wave" phenomenon that appeared before the second limiting current and this new "wave" was demonstrated to be related to the direct reduction of both hydrate of SO_2 and bisulfite on the steel surface.

Keywords: CCUS; CO_2; SO_2; cathodic reaction; 316L stainless steel

1. INTRODUCTION

Carbon capture, utilization and storage (CCUS) is regarded as an effective way to reduce CO_2 emissions from emission sources, such as coal-fired power plants and refineries. One CO_2 utilization form is that captured CO_2 is transported to an oil field to enhance oil recovery (EOR) before permanent geological storage, which can compensate for the cost of the capture, transport and storage steps. In coal-fired power plants, NO_2, SO_2, O_2, H_2O and other impurities are inevitably mixed with the captured CO_2 [1, 2]. Impurities in supercritical CO_2 streams pose a huge challenge to the integrity of pipeline equipment during the transport process.

The issue of steel corrosion in supercritical CO_2 environments containing various impurities has already been widely investigated [3-22]. SO_2 is one of the major impurities during the CO_2 capture process and can result in severe corrosion of pipeline steel owing to the formation of hydrate of SO_2 and sulfuric acid. Choi [3] found that when 1% SO_2 was added to a water-saturated supercritical CO_2 system, the corrosion rate of X65 steel increased from 0.38 to 5.6 mm/y, and γ-$FeSO_3 \cdot 3H_2O$ was observed in product scales, which has poorer protectiveness to the substrate compared to $FeCO_3$. When O_2 and SO_2 were present together, the corrosion rate of X65 steel reached 7 mm/y. Xiang [4] reported that the addition of 0~2.0% SO_2 in a water-saturated supercritical CO_2 system resulted in a corrosion rate variation of X70 steel from 0.056 to 0.88 mm/y. Hua [6] determined that the addition of SO_2 and O_2 impurities in water-saturated supercritical CO_2 accelerated the uniform corrosion rate of X65 carbon steel from 0.1 mm/y to 0.7 mm/y and localized corrosion became more severe with rising SO_2 concentrations. Although the corrosion behaviors of steels in atmospheric environments [23-25] and in supercritical CO_2 environments with SO_2 impurities have been studied extensively, the electrochemical behaviors of steel corrosion in supercritical CO_2/SO_2 environments still merits further investigation.

Investigation of corrosion behaviors of steels in weak acid environments is currently a hot research topic. Tran [26] evaluated the corrosion behavior of mild steel in carbonic and acetic acid solutions and concluded that carbonic and acetic acid mainly act via a “buffer effect” mechanism: only hydrogen ions were supplied by these weak acids during the cathodic process. Kahyarian [27] also look at the corrosion mechanism of acetic acid and obtained similar results. Zheng [28-31] reviewed the corrosion behavior of pipeline steel in H_2S- and CO_2/H_2S-containing solution, proposing a H_2S “direct reduction” mechanism - the direct reduction of H_2S molecules during the cathodic process [28]:

$$2H_2S + 2e^- \rightarrow H_2(g) + 2HS^- \quad (1)$$

Recently, Xiang [32] studied the corrosion behavior of valve steel in a CO_2/SO_2 solution and hydrate of SO_2 or bisulfite were considered to be directly involved in the cathodic reaction. However, whether hydrate of SO_2, bisulfite or both of them are directly reduced during the reactions still needs further verification.

In this work, the corrosion behavior of 316L austenitic stainless steel in a CO_2-SO_2-H_2O mixture was studied by adding different amount of SO_2 to the test solution under atmospheric pressure in order to validate whether the previous direct reduction mechanism depended on the working electrode material and further determine if hydrate of SO_2, bisulfite or both are directly reduced in the cathodic reaction. Potentiodynamic sweep, linear polarization resistance (LPR) and electrochemical impedance spectroscopy (EIS) methods were applied.

2. EXPERIMENTAL PROCEDURE

2.1 Materials and pretreatment

The working electrodes were made of 316L austenitic stainless steel. The chemical composition of this steel was as follows (by wt.%): C, 0.013; Si, 0.07; Mn, 0.06; P, 0.023; Mo, 2.30; Cr, 17.14; Ni, 12.65; S, 0.075 and Fe in balance. During the experiments, the working electrode was machined from this steel and mounted in epoxy resin with a working surface area of 0.78 cm^2. The working surface was polished with a series of silicon carbide papers progressively up to 600 grit, and

then washed with acetone to remove surface contaminations and dehydrated by absolute ethanol. All working electrodes were dried in a vacuum oven for 24 h before tests. A SO_2 solution (manufactured by Aladdin Ltd.) was employed in the tests, simulating the SO_2 impurity in the CO_2 stream.

2.2 Experimental setup

The experimental setup is illustrated in Figure 1. The experiment was carried out under atmospheric pressure at 25 °C by using a 3 L glass cell. The electrolyte solution was a 1 wt.% sodium sulfate (Na_2SO_4) solution. The electrochemical measurements used a standard three-electrode experimental setup. A saturated calomel (Hg/Hg_2Cl_2) reference electrode was utilized and connected by a Luggin capillary. A platinum plate was used as the counter electrode. The solution pH value was measured with a pH meter (Mettler Toledo, FE20). A potentiostat (Gamry, Reference 3000) was used for electrochemical tests. Before each test, high-purity (99.999 vol.%) N_2 was purged through the solution for at least 2 h to remove oxygen. High-purity CO_2 (99.999 vol.%) was purged through the solution to reach CO_2-saturated condition, and then 100 or 1,000 ppmw of SO_2 was added to the solution depending on the test conditions. High-purity CO_2 or N_2 was continuously purged through the solution at a relatively low flow rate during the test depending on the test conditions. The pH value of solution was adjusted by sulfuric acid (H_2SO_4), sodium hydroxide (NaOH) or sodium bisulfite ($NaHSO_3$) to the desired value. An exhaust treatment tower was made use of for exhaust gas treatment. All the tests were carried out under static conditions. The detailed test conditions are listed in Table 1.

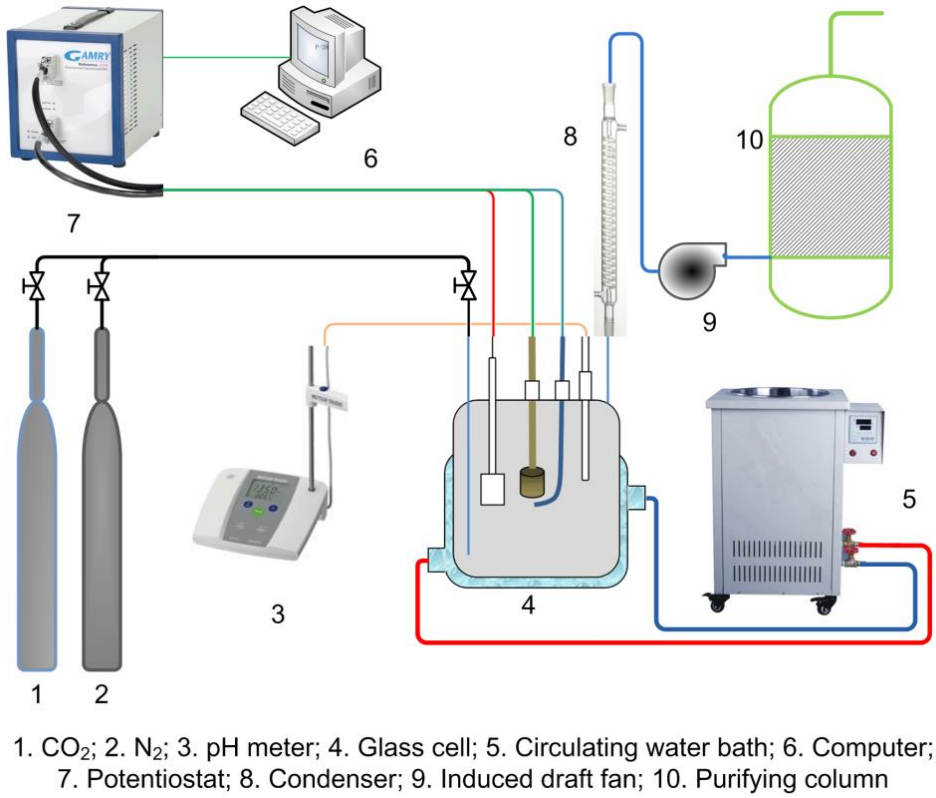

Figure 1. Schematic diagram of the setup for electrochemical measurements.

Table 1. Test conditions

Test No.	Temperature (°C)	pH	CO_2 partial pressure (bar)	SO_2 concentration (ppmw)	$NaHSO_3$ concentration (ppmw)
1	25	1	0.97	1,000	0
2		2	0.97	0	
3		2	0.97	100	
4		3	0.97	0	
5		3	0.97	100	
6		3	0.97	1,000	
7		4	0.97	0	
8		4	0.97	100	
9		4	0	100	
10		4	0.97	100	26,000

2.3 Methods

Polarization resistance (R_p) was measured by polarizing the working electrode ±10 mV around the open circuit potential (OCP) with a scanning rate of 0.2 mV/s. EIS tests were conducted around the OCP of ±5 mV with a frequency range from 10^4 to 10^{-2} Hz. Potentiodynamic sweeps were carried out to establish the behavior of cathodic reactions with a scanning rate of 0.2 mV/s. The solution resistances were obtained by EIS tests and the polarization curves were corrected accordingly. The corrosion current density (i_{corr}) was calculated by Equation (2) [33] and the corrosion rate was obtained according to Equation (3) [34]:

$$i_{corr} = \frac{B}{R_P} = \frac{b_a \times b_c}{2.3 \times R_p \times (b_a + b_c)} \tag{2}$$

$$Corrosion\ Rate\ (\text{mm/y}) = \frac{0.00327 \times i_{corr}\ (\mu\text{A/cm}^2) \times EW\ (\text{g})}{Density\ (\text{g/cm}^3)} \tag{3}$$

where b_a is the anode tafel slope in mV/dec and b_c is the cathode tafel slope in mV/dec. *EW* is the equivalent weight in grams. The *B* value was 24 mV/dec, which was determined based on the experimental measurement results.

3. RESULTS AND DISCUSSION

Figure 2 depicts the cathodic polarization curves of 316L stainless steel in a CO_2-saturated solution with and without SO_2 at pH 4.0. When 100 ppmw SO_2 appeared in the CO_2-saturated solution, the cathodic polarization curve shifted to the right, indicating that the addition of SO_2 might promote cathodic reactions. The concentration of SO_2 stands for the concentration of hydrate of SO_2 with one H_2O.

The change of the limiting current may be affected by the diffusion of SO_2 or bisulfite from the bulk to metal surface. The final stage of the cathodic polarization curves were mainly controlled by the

reduction of water. When only 100 ppmw SO_2 was added to 1 wt.% Na_2SO_4 solution without CO_2, the cathodic polarization curve with 100 ppmw SO_2 only was significantly different from the cases with CO_2. It can be speculated that the cathodic reactions in CO_2-saturated solution differ from that with 100 ppmw SO_2 exclusively. The limiting current for the case with only 100 ppmw SO_2 was lower than that with just CO_2. This may indicate that H_2CO_3 and HCO_3^- were directly involved in the cathodic reactions that resulted in a higher limiting current than the case with 100 ppmw SO_2 only. These results might also imply that there was a synergistic effect between CO_2 and SO_2.

$NaHSO_3$ was also used to adjust the solution pH to 4.0 without using NaOH after adding 100 ppmw SO_2 to the CO_2-saturated solution, and the amount of $NaHSO_3$ was 26,000 ppmw. When a large amount of $NaHSO_3$ was present, the charge transfer current was further increased and no limiting current was observed in the test potential range. The cathodic process was mainly controlled by the charge transfer process. HSO_3^- ions may be directly involved in the cathodic reaction.

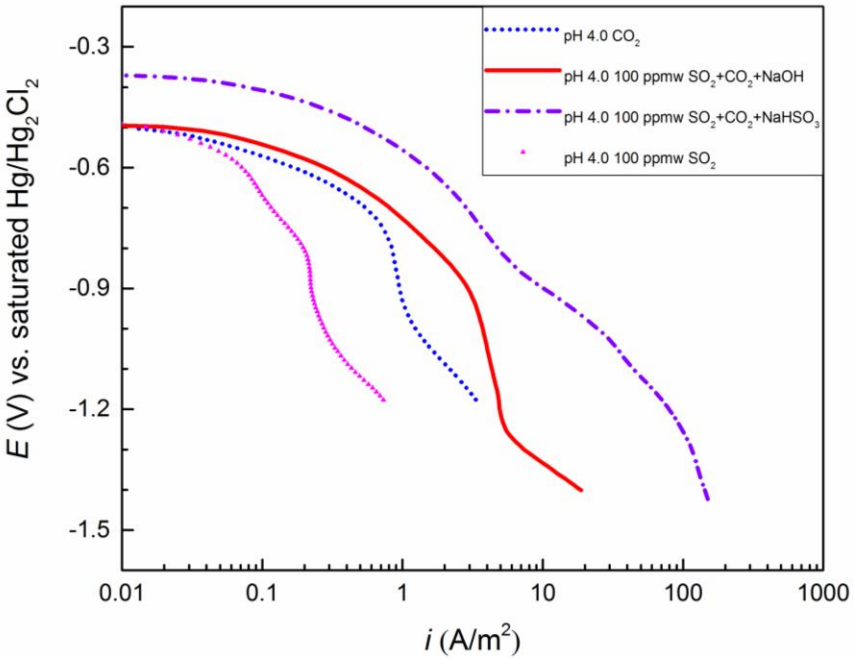

Figure 2. Comparison of polarization curves of 316L stainless steel under different conditions at 25 °C with a pH 4.0 in aqueous solution with saturated CO_2 and 1 wt.% Na_2SO_4.

The cathodic polarization curves of 316L stainless steel in a CO_2-saturated solution with different amounts of SO_2 at pH 3.0 are portrayed in Figure 3. The cathodic polarization curve of the case with 100 ppmw SO_2 at pH 3.0 also shifted to the right, indicating that SO_2 promoted cathodic reactions. The addition of SO_2 enhanced the charge transfer current and limiting currents and a "second wave" appeared before the second limiting current. This phenomenon is similar to what was seen by Zheng [28] with their work on a H_2S corrosion mechanism. This new "wave" that appeared may be based on the fact that hydrate of SO_2 or bisulfite was directly involved in the cathodic reactions. The previously proposed direct reduction mechanism was [32]:

$$2SO_2 + H_2O + 2e^- \rightarrow H_2 + 2HSO_3^- \quad (4)$$

or:

$$2HSO_3^- + 2e^- \rightarrow H_2 + 2SO_3^{2-} \quad (5)$$

At pH 3.0, the cathodic polarization curves of 316L stainless steel in CO_2-saturated solution with SO_2 involved the direct reduction of hydrate of SO_2 (and/or bisulfite), reduction of H^+ and H_2O. There were two limiting currents and a "second wave" in the polarization curve for the case with 100 ppmw SO_2 under pH 3.0 conditions. The first limiting current of the polarization curve for the case with 100 ppmw SO_2 is close to the limiting current platform of a CO_2-saturated solution without SO_2, and we deduced that this diffusion current mainly reflects the diffusion of H^+, H_2CO_3 and HCO_3^-. The "second wave" reflects the diffusion of SO_2 or bisulfite, besides H^+, H_2CO_3 and HCO_3^-. The final stage of the cathodic sweep was the reduction of H_2O.

When 1,000 ppmw SO_2 was added to the CO_2-saturated solution at pH 3.0, the same "second-wave" phenomenon appeared on the cathodic polarization curve, and this curve further shifted to the right. OCP rose with the increase of SO_2 concentration. As the concentration of SO_2 increases, if only hydrogen ions are involved in the cathodic reaction, the charge transfer current should remain the same. As seen, when the amount of SO_2 is elevated, the cathodic polarization curve entirely shifted to the right, which has the same results as the previous study that employed X80CrSiMoW152 valve steel as the working electrode [32]. A similar analysis was also found when analyzing the corrosion mechanism of mild steel in acetic acid [26].

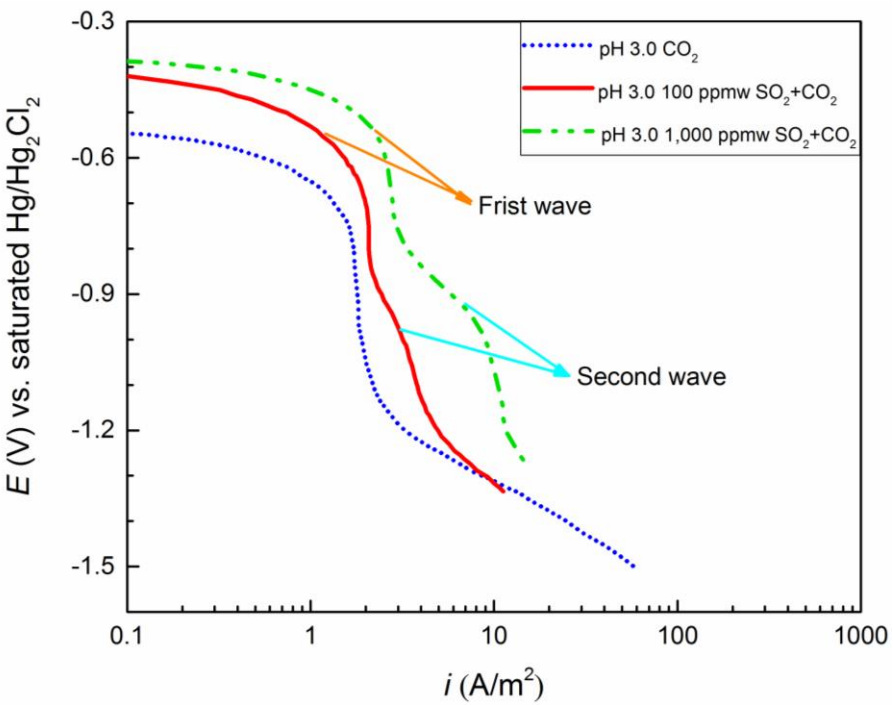

Figure 3. Comparison of polarization curves of 316L stainless steel with different amounts of SO_2 at 25 °C with a pH 3.0 in aqueous solution with saturated CO_2 and 1 wt.% Na_2SO_4.

Figure 4 exhibits the cathodic polarization curves of 316L stainless steel in a CO_2-saturated solution with and without SO_2 at pH 2.0. The shape of the cathodic polarization curve had no obvious change when SO_2 was present. At pH 4.0, the concentration of H^+ ions was limited in solution, hence

the direct reduction of hydrate of SO_2 or bisulfite dominated the change of charge transfer current and the limiting diffusion current. At pH 3.0, more hydrogen ions were required and additional H_2SO_4 was added to provide additional H^+ ions to reach the desired pH. The contribution of H^+ ions and hydrate of SO_2 or bisulfite to the cathodic reactions was at the comparative level. At pH 2.0, the concentration of H^+ ions in the solution was high and H^+ reduction was dominant during the whole cathodic process while 100 ppmw SO_2 played a very small role in cathodic reactions. The limiting current of hydrate of SO_2 or bisulfite was obscured by the limiting current of hydrogen ions.

We also calculated the water chemistry and determined the component concentrations in order to further identify the direct reduction of hydrate of SO_2 or bisulfite based on the following equations:

$$c(SO_2) = \frac{c(HSO_3^-) \cdot c(H^+)}{K_1} \tag{6}$$

$$c(HSO_3^-) = \frac{c(SO_3^{2-}) \cdot c(H^+)}{K_2} \tag{7}$$

$$c[S(IV)] = c(SO_2) + c(HSO_3^-) + c(SO_3^{2-}) \tag{8}$$

where the K_1 and K_2 are the first and second ionization equilibrium constants of hydrate of SO_2, respectively. The values of K_1 and K_2 were 1.39×10^{-2} and 6.72×10^{-8} mol/kg at 25 °C, respectively [35].

The calculated component concentrations are listed in Table 2. This calculation ignored the impact of CO_2 and Na_2SO_4 on the ionization balance of hydrate of SO_2 while the presence of SO_2 can inhibit the dissociation of H_2CO_3 [21]. For the cases in CO_2-saturated solution with 100 ppmw SO_2 at pH 4.0 and pH 3.0, there was a 5.65% decrease in bisulfite concentration when the pH value decreased from 4.0 to 3.0. However, under the conditions of pH 3.0 and pH 4.0, the concentration of SO_2 in the solution was very low and had an order of magnitude difference. For the water chemistry calculation under supercritical CO_2 environment with impurities, the work by Sun [21] can be referred to.

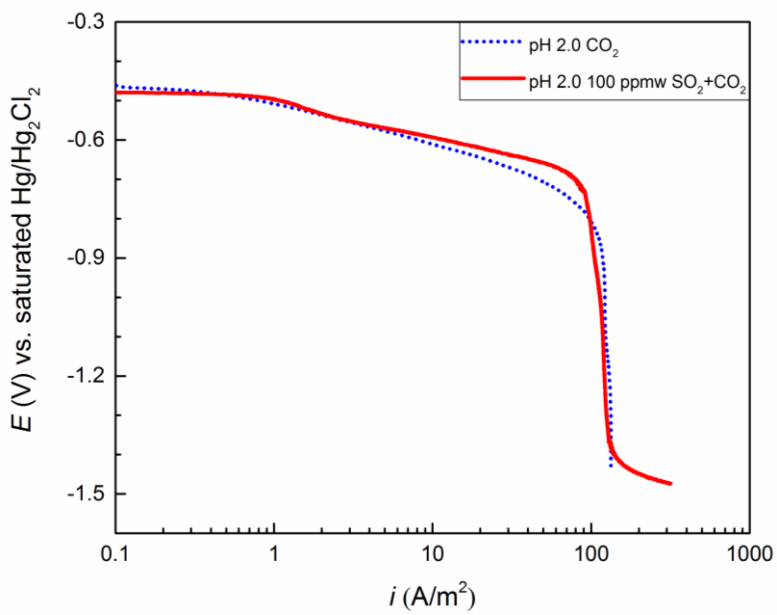

Figure 4. Comparison of polarization curves of 316L stainless steel with and without 100 ppmw SO_2 at 25 °C with a pH 2.0 in aqueous solution with saturated CO_2 and 1 wt.% Na_2SO_4.

Table 2. Results from calculating component concentrations in solution.

No.	pH	Temperature, °C	$c[S(IV)]$, mol/L	$c(HSO_3^-)$, mol/L	$c(SO_2)$, mol/L	$c(SO_3^{2-})$, mol/L
1	4	25	$1.25\cdot10^{-06}$ (100 ppmw)	$1.24\cdot10^{-06}$	$8.92\cdot10^{-09}$	$8.33\cdot10^{-10}$
2	3	25	$1.25\cdot10^{-06}$ (100 ppmw)	$1.17\cdot10^{-06}$	$8.39\cdot10^{-08}$	$7.84\cdot10^{-11}$
3	3	25	$1.25\cdot10^{-05}$ (1,000 ppmw)	$1.17\cdot10^{-05}$	$8.39\cdot10^{-07}$	$7.84\cdot10^{-10}$
4	2	25	$1.25\cdot10^{-06}$ (100 ppmw)	$7.27\cdot10^{-07}$	$5.23\cdot10^{-07}$	$4.89\cdot10^{-12}$
5	1	25	$1.25\cdot10^{-05}$ (1,000 ppmw)	$1.53\cdot10^{-06}$	$1.10\cdot10^{-05}$	$1.03\cdot10^{-12}$

Figure 5 shows the cathodic polarization curves of 316L stainless steel in CO_2-saturated solution with 1 wt.% Na_2SO_4 under different pH conditions. The shape of the cathodic polarization curves is the same as that obtained by Tran [26], which also showed that with the decrease of pH, the charge transfer current increased and the limiting current rose. This result verified the reliability of this experimental study.

The cathodic polarization curves of 316L stainless steel in CO_2-saturated solution containing SO_2 at different pH conditions are depicted in Figure 6. The second limiting current of the case in CO_2-saturated solution with 100 ppmw SO_2 at pH 4.0 had a small increase compared with that in CO_2-saturated solution with 100 ppmw SO_2 at pH 3.0. The concentration of bisulfite in the case of CO_2-saturated solution with 100 ppmw SO_2 at pH 4.0 was a little larger than that with CO_2-saturated solution with 100 ppmw SO_2 at pH 3.0. This consistency implies that the second limiting current was mainly related to the direct reduction and limiting diffusion of bisulfite ions.

The cathodic polarization curve of the case in CO_2-saturated solution with 1,000 ppmw SO_2 at pH 1.0 is also shown in Figure 6. At pH 1.0, the cathodic current was large, and the solution resistance was deducted from the cathodic sweeps, leading to a smaller scan range as found in Figure 6. However, the “second-wave” phenomenon was also observed. The first-stage limiting current for the case at pH 1.0 was close to the second-stage limiting current of the case with CO_2-saturated solution with 1,000 ppmw SO_2 at pH 3.0. The concentration of bisulfite in the case of CO_2-saturated solution with 1,000 ppmw SO_2 at pH 3.0 was close to the concentration of SO_2 in the case of CO_2-saturated solution with 1,000 ppmw SO_2 at pH 1.0. Further, at pH 1.0, the first-stage limiting current was most possibly related to the limiting diffusion of SO_2 while the second-stage limiting current was predominantly attributed to the limiting diffusion of H^+ ions. This characteristic is different from the cases at other pH value conditions.

Based on these test results, we concluded that hydrate of SO_2 and bisulfite are both involved in cathodic reactions. This can readily explain the aforementioned characteristics of cathodic curves under all pH conditions. However, if O_2 was also involved in the CO_2 stream, the oxidation of bisulfite may alter this reaction behavior.

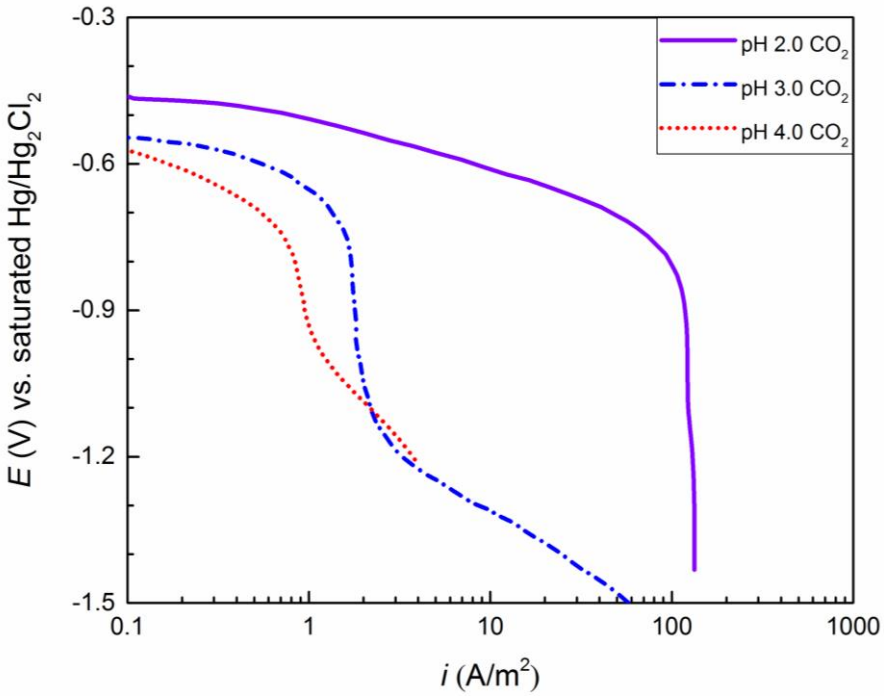

Figure 5. Comparison of potentiodynamic curves of 316L stainless steel for different pH values at 25 °C in aqueous solution with saturated CO_2 and 1 wt.% Na_2SO_4.

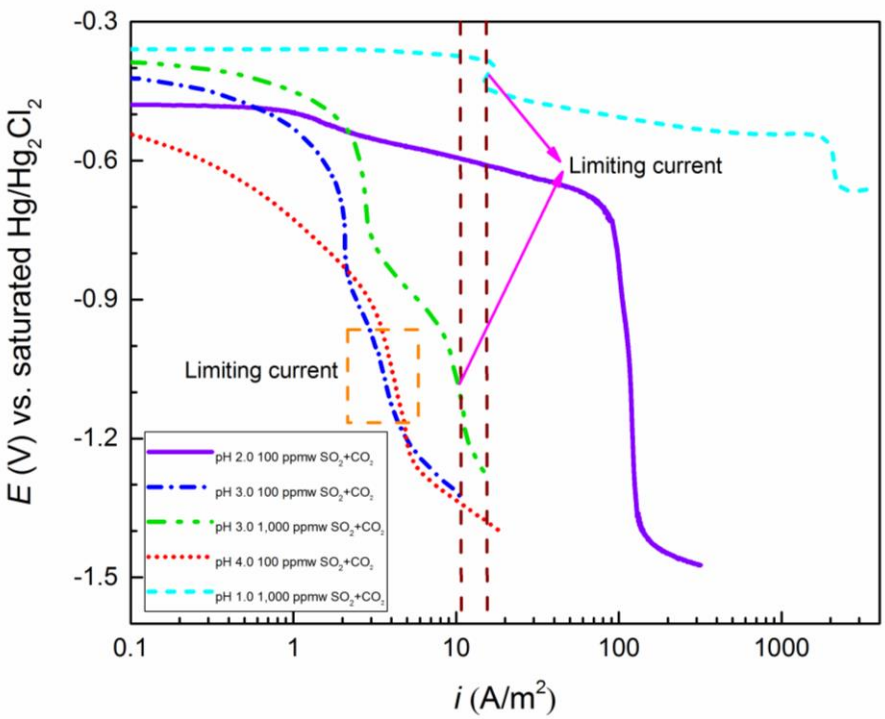

Figure 6. Comparison of potentiodynamic curves of 316L stainless steel with SO_2 for different pH values at 25 °C in aqueous solution saturated with CO_2, 1 wt% Na_2SO_4.

Figure 7 portrays the corrosion rates obtained by the LPR method under different test conditions. Typically, the corrosion rates increased when SO_2 appeared in the CO_2-saturated solution

at the same pH. The corrosion rate in the case of CO_2-saturated solution with 100 ppmw SO_2 is approximately eight times the corrosion rate of the case with CO_2-saturated solution without SO_2 at pH 2.0. It can be thought that although SO_2 had a marginal effect on the cathodic polarization curve at pH 2.0, it could promote the anodic reaction, which has been demonstrated by previous work [32]. The experimental results of steel corrosion in supercritical CO_2 environments with SO_2 impurities also verified that the addition of SO_2 impurities can increase the corrosion rates [3-5]. At pH 3.0 and pH 4.0, all the corrosion rates were less than 0.1 mm/y and no visible corrosion took place on the steel surface after tests, implying the weak corrosiveness of the test solutions. At pH 3.0, the corrosion rate increases with the rise in SO_2 concentration. The corrosion rate of the case with CO_2-saturated solution without SO_2 at pH 4.0 was minimal, specifically as low as 0.0013 mm/y.

The results of EIS tests for different conditions at pH 4.0 are demonstrated in Figure 8. The polarization resistance of the case with CO_2-saturated solution without SO_2 seems to be the largest and the Warburg impedance was found in all cases, potentially indicating the formation of product films that can impede the diffusion of corrosive media. The composition of corrosion products might be complex if O_2 was involved in the corrosion process [36]. The overall trend of polarization resistance obtained by EIS was in robust agreement with the LPR test results.

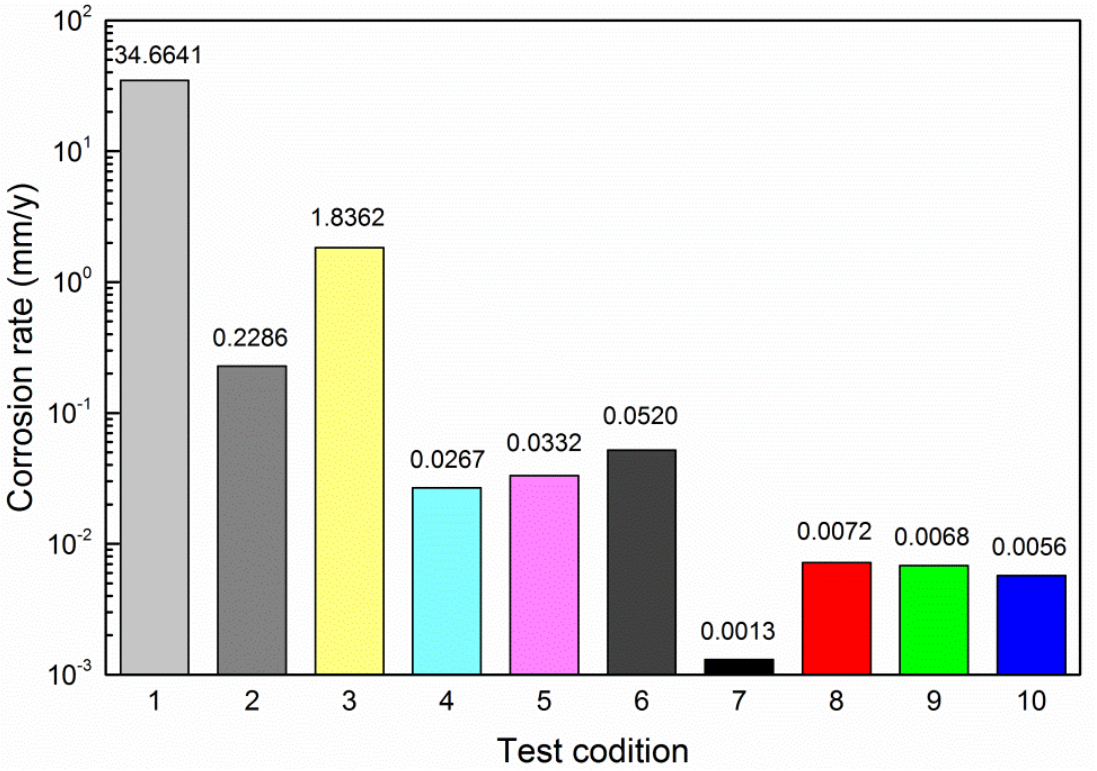

Figure 7. Comparison of electrochemical measurement results of 316L stainless steel under different test conditions. The test condition numbers correspond to the condition numbers listed in Table 1: 1. pH 1.0, CO_2 + 1,000 ppmw SO_2; 2. pH 2.0, CO_2; 3. pH 2.0, CO_2 + 100 ppmw SO_2; 4. pH 3.0, CO_2; 5. pH 3.0, CO_2 + 100 ppmw SO_2; 6. pH 3.0, CO_2 + 1,000 ppmw SO_2; 7. pH 4.0, CO_2; 8. pH 4.0, CO_2 + 100 ppmw SO_2; 9. pH 4.0, 100 ppmw SO_2; 10. pH 4.0, CO_2 + 100 ppmw SO_2 + $NaHSO_3$.

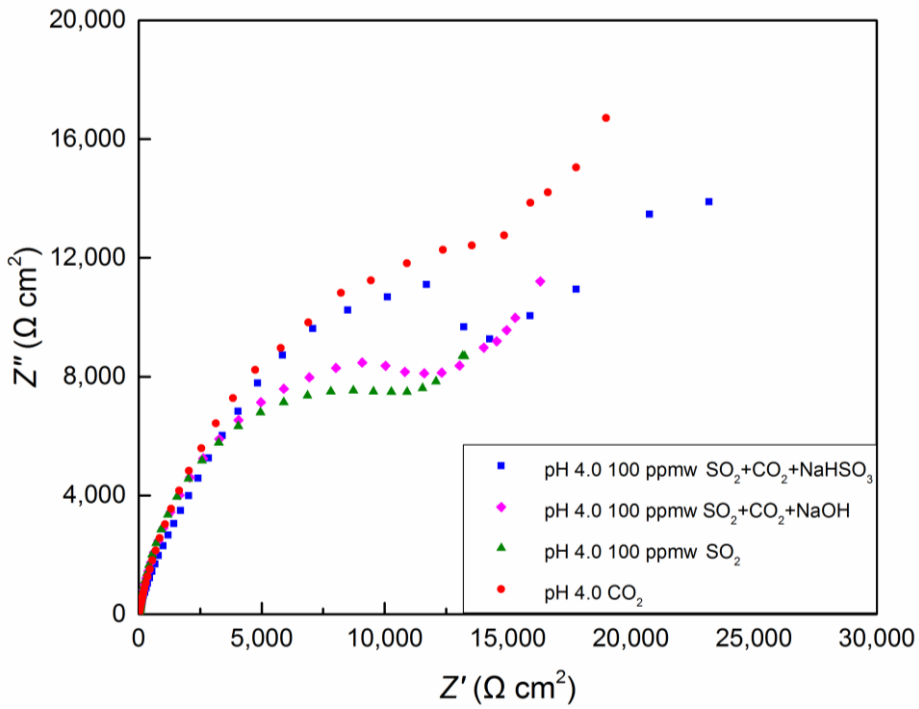

Figure 8. Nyquist plots at 0 V vs. a saturated Hg/Hg_2Cl_2 electrode of 316L stainless steel under different test conditions at 25 °C in aqueous solution with saturated CO_2 and 1 wt% Na_2SO_4.

4. CONCLUSIONS

In the present work, the cathodic reaction behavior of 316L stainless steel corrosion in a mixed CO_2-SO_2-H_2O environment was assessed. The potentiodynamic sweep, LPR and EIS methods were applied experimentally. The following conclusions can be drawn based on the test results:

(1) The presence of SO_2 increased the corrosion rate at the same pH, especially for the cases at lower pH conditions;

(2) There was no visible corrosion observed in the presence or absence of SO_2 in the CO_2-saturated solution at pH 4.0 and 3.0;

(3) When SO_2 appeared in CO_2-saturated solution, the cathodic reactions were affected. New cathodic reactions were involved in the cathodic process; and

(4) Both hydrate of SO_2 and bisulfite are directly reduced on the steel surface during the cathodic process, and this is besides the H^+ reduction taking place.

ACKNOWLEDGEMENTS
The authors would like to announce that this work was financially supported by National Natural Science Foundation of China (51604289), National Key R&D Program of China (2017YFC0805800), Beijing Natural Science Foundation (2172048) and Science Foundation of China University of Petroleum, Beijing (2462014YJRC043). Part of the results was presented in the conference of Eurocorr 2017, and permission to publish these results has been obtained.

References

1. A.Oosterkamp and J. Ramsen, State-of-the-art overview of CO_2 pipeline transport with relevance to offshore pipelines, POLYTEC, 2008.
2. E. de Visser, C. Hendriks, M. Barrio, M.J. Molnvik, G. de Koeijer, S. Liljemark and Y. Le Gallo, *Int. J. Greenh. Gas Con.*, 2 (2008) 478.
3. Y.S. Choi, S. Nesic and D. Young, *Environ. Sci. Technol.*, 44 (2010) 9233.
4. Y. Xiang, Z. Wang, C. Xu, C. Zhou, Z. Li and W. Ni, *J. Supercrit. Fluid.*, 58 (2011) 286.
5. Y. Hua, R. Barker and A. Neville, *Int. J. Greenh. Gas Con.*, 37 (2015) 412.
6. Y. Hua, R. Barker and A. Neville, *Corrosion*, 71 (2015) 667.
7. Y. Hua, R. Barker and A. Neville, *Int. J. Greenh. Gas Con.*, 31 (2014) 48.
8. Y. Hua, R. Barker and A. Neville, *J. Supercrit. Fluid.*, 97 (2015) 224.
9. F. Farelas, Y.S. Choi and S. Nešić, *Corrosion*, 69 (2013) 243.
10. M. Xu, Q. Zhang, X. Yang, Z. Wang, J. Liu and Z. Li, *J. Supercrit. Fluid.*, 107 (2016) 286.
11. L. Wei, X. Pang and K. Gao, *Corros. Sci.*, 103 (2016) 132.
12. L. Wei, X. Pang and K. Gao, *Corros. Sci.*, 111 (2016) 637.
13. C. Sun, J. Sun, Y. Wang, X. Lin, X. Li, X. Cheng and H. Liu, *Corros. Sci.*, 107 (2016) 193.
14. C. Sun, Y. Wang, J. Sun, X. Lin, X. Li, H. Liu and X. Cheng, *J. Supercrit. Fluid.*, 116 (2016) 70.
15. J. Sun, C. Sun, G. Zhang, X. Li, W. Zhao, T. Jiang, H. Liu, X. Cheng and Y. Wang, *Corros. Sci.*, 107 (2016) 31.
16. A. Dugstad, M. Halseid and B. Morland, *Energ. Procedia*, 37 (2013) 2877.
17. A.S. Ruhl and A. Kranzmann, *J. Supercrit. Fluid.*, 68 (2012) 81.
18. S. Sim, I.S. Cole, F. Bocher, P. Corrigan, R.P. Gamage, N. Ukwattage and N. Birbilis, *Int. J. Greenh. Gas Con.*, 17 (2013) 534.
19. Y. Xiang, Z. Long, C. Li, H. Huang and X. He, *Int. J. Greenh. Gas Con.*, 63 (2017) 141.
20. Y. Xiang, M. Xu and Y.-S. Choi, *Corros. Eng. Sci. Techn.*, 52 (2017) 485.
21. J. Sun, C. Sun and Y. Wang, *Ind. Eng. Chem. Res.*, doi: 10.1021/acs.iecr.7b04870 (2018).
22. M. Xu, W. Li, Y. Zhou, X. Yang, Z. Wang and Z. Li, *Int. J. Greenh. Gas Con.*, 51 (2016) 357.
23. W. Lv, C. Pan, W. Su, Z. Wang, S. Liu and C. Wang, *Corros. Eng. Sci. Techn.*, 51 (2016) 155.
24. S. Sabir and A.A. Ibrahim, *Corros. Eng. Sci. Techn.*, 52 (2017) 276.
25. I.M. Allam, J.S. Arlow and H. Saricimen, *Corros. Sci.*, 32 (1991) 417.
26. T. Tran, Corrosion mechanisms of mild steel in weak acids, Ohio University, 2014.
27. A. Kahyarian, B. Brown and S. Nešić, *Corrosion*, 72 (2016) 1539.
28. Y. Zheng, B. Brown and S. Nešić, *Corrosion*, 70 (2014) 351.
29. Y. Zheng, J. Ning, B. Brown and S. Nešić, *Corrosion*, 71 (2015) 316.
30. Y. Zheng, J. Ning, B. Brown and S. Nešić, *Corrosion*, 72 (2016) 1519.
31. Y. Zheng, J. Ning, B. Brown and S. Nešić, *Corrosion*, 72 (2016) 679.
32. Y. Xiang, C. Li, Z. Long, C. Guan, W. Wang and W. Hesitao, *Electrochim. Acta*, 258 (2017) 909.
33. M. Stern and A.L. Geary, *J. Electrochem. Soc.*, 104 (1957) 56.
34. S.W. Dean, Handbook on Corrosion Testing and Evaluation, John Wiley, (1971) New York.
35. R.N. Goldberg and V.B. Parker, *J. Res. National Bur. Stand.*, 90 (1985) 341.
36. W. McLeod and R.R. Rogers, *Corrosion*, 22 (1966) 143